Agricultural and Forest Meteorology 256–257 (2018) 196–206

Contents lists available at ScienceDirect

Agricultural and Forest Meteorology

journal homepage: www.elsevier.com/locate/agrformet

Stage-dependent temperature sensitivity function predicts seed-setting rates under short-term extreme heat stress in rice

Ting Sun[a,b], Toshihiro Hasegawa[b], Liang Tang[a], Wei Wang[a], Junjie Zhou[a], Leilei Liu[a], Bin Liu[a], Weixing Cao[a], Yan Zhu[a,*]

[a] National Engineering and Technology Center for Information Agriculture, Key Laboratory for Crop System Analysis and Decision Making, Ministry of Agriculture, Jiangsu Key Laboratory for Information Agriculture, Jiangsu Collaborative Innovation Center for Modern Crop Production, Nanjing Agricultural University, Nanjing, Jiangsu, 210095, PR China

[b] Agro-Environmental Research Division, Tohoku Agricultural Research Center, National Agricultural and Food Research Organization (NARO), 4 Akahira, Shimokuriyagawa, Morioka, 020-0198, Japan

ARTICLE INFO

Keywords:
Heat stress
Rice
Seed-setting rate
Growth stage
Modelling

ABSTRACT

Seed-setting rate of rice (*Oryza sativa* L.) significantly decreases under high temperatures during the reproductive period largely due to heat-induced spikelet sterility. The effects depend largely on the timing and severity of heat stress, but the variation in the sensitivity of seed-setting rate in response to heat stress at different growth stages is not yet well simulated by most of the present crop models. To investigate the quantitative relationships between seed-setting rates of rice and various exposures of heat stress, we conducted four-year phytotron experiments with four different temperature regimes (the target maximum/minimum temperatures, 32 °C/22 °C, 35 °C/25 °C, 38 °C/28 °C and 41 °C/31 °C in 2011 and 2012; 32 °C/22 °C, 36 °C/26 °C, 40 °C/30 °C and 44 °C/34 °C in 2014 and 2015) with factorial combinations of durations (2, 4 and 6 days in 2014 and 2015; 3, 5 and 7 days in 2011; 3, 6 and 9 days in 2012) and the timings (0, 6 or 12 days after flowering), using three japonica cultivars. The duration and intensity of heat stress were quantified by the heat degree-days (HDD), defined as the temperature sum above a critical temperature value, which varied from 35 to 36 °C, depending on the cultivars. The observed seed-setting rates were well expressed as a logistic function of HDD, but the temperature sensitivity parameter varied with the timing of heat stress and the spikelet positions on the panicle. The variation in timing of flowering was apparent among upper, middle and lower parts of the panicles: 1 and 3-day delay of flowering for the spikelets on the middle and lower parts of the panicles, respectively, compared with upper ones. We therefore developed a simulation model that reflects the changes in the sensitivity of seed-setting rate to HDD to estimate the effects of heat stress with different intensities or durations at any time from flowering onward. The model with the stage-dependent parameters improved substantially the root mean square error (RMSE) and mean bias error (MBE) of seed-setting % from 20.1 and 6.0 to 7.6 and 0.2, respectively, compared to that with the stage-independent parameters. The proposed model needs to be tested under field conditions, but will be an important basis for accurate prediction of seed-setting rates in rice, which is critical for reliable estimates of crop production under climate change.

1. Introduction

Rice is one of the world's most important cereals as the staple food for the majority of the world population. Heat stress events, which caused large negative impacts on rice yields, have been reported in main global rice production areas such as Southern Asia (Aggarwal and Mall, 2002; Ishimaru et al., 2016; Matsushima et al., 1983; Osada et al., 1973), East Asia (Hasegawa et al., 2009; Yawei and Hua, 2006) and Southeast Asia (Wassmann et al., 2009). Therefore, rice plants are potentially at high risk of exposure to heat stress because the short episodes of extreme temperature will become more frequent with the increasing variability and intensity of global warming (IPCC, 2013; Tebaldi et al., 2006).

Crop growth model is the most important tool to predict rice productivity under different climate scenarios, but recent multi-models comparisons demonstrated that large uncertainties are involved in predictions by individual crop models (Asseng et al., 2013; Li et al., 2015). The uncertainties are largely associated with predictions under

* Corresponding author.
E-mail address: yanzhu@njau.edu.cn (Y. Zhu).

https://doi.org/10.1016/j.agrformet.2018.03.006
Received 15 September 2017; Received in revised form 16 February 2018; Accepted 5 March 2018
Available online 20 March 2018
0168-1923/

extreme temperatures, because most of the current crop models were developed under current temperature ranges. Although some crop models were tested under extreme high temperature conditions, variation in crop yield under largely varying temperatures is still difficult to predict (Liu et al., 2016; Shi et al., 2015a, b; Wang et al., 2017). It is therefore imperative to improve the quantitative understandings on the crop responses to extreme temperatures, which are projected to increase greatly under projected changes in climate.

Heat stress occurs when the temperature rises above a threshold value and persists over a certain period of time, and results in an irreversible damage on crop plants (Wahid et al., 2007). Various growth processes can be affected by heat stress, but the sensitivity and severity of the stresses changes depending on the growth stages and processes (Sánchez et al., 2014). Among them, the seed-setting rate is highly sensitive to heat stress, and directly influences grain yield via reduced number of filled grains (Siebert et al., 2014). A pioneering study by Satake and Yoshida (1978) identified the most sensitive stage for seed-setting as around flowering. Horie (1993) showed that the seed-setting rate decreases sharply above around 35 °C using temperature gradient chambers. Since then, this threshold temperature has been widely used in rice growth models (Bouman, 2001; Shi et al., 2015a, b; Tang et al., 2009). However, as shown in many chamber and field studies, 35 °C is not an unequivocal threshold temperature for failure in seed-setting (Hasegawa et al., 2011; Jagadish et al., 2007; Satake and Yoshida, 1978; Tian et al., 2010), which needs further examination (Sánchez et al., 2014).

Duration of high-temperature exposure is another important determinant of the effects of heat stress. For instance, seed-setting rate was almost linearly decreased as duration of high-temperature exposure increased from 0 to 5 h, because of increased spikelet sterility (Jagadish et al., 2007). At higher temperatures, the critical duration to induce equal sterility became shorter (Satake and Yoshida, 1978). This suggests that a cumulative temperature above a threshold value seemed to be more reasonable because of the interaction between temperature intensity and duration (Liu et al., 2014; Prasad et al., 1999; Shi et al., 2015a, b). Nevertheless, heat-induced spikelet sterility was generally quantified with the daily maximum temperature (Bouman, 2001; Horie et al., 1996; Krishnan et al., 2007; Matthews, 1995; Nakagawa et al., 2003; Shi et al., 2016; Tang et al., 2009). This may be because determination of the threshold temperatures and/or the response of seed-setting to the heat dose have not been well documented.

Early studies clearly demonstrated that susceptibility to heat damages peaks at the heading stage and decreases sharply from then onward for an individual panicle (Satake and Yoshida, 1978). The rice community, however, includes panicles and spikelets at different growth stages. Timing of panicle exertion varies among tillers in the field by 10–14 days and flowering time of spikelets even on the same panicle can vary by 7–10 days (Yoshida, 1981). On the other hand, heat events with different intensities and duration can occur at any time during reproductive stages (Hasegawa et al., 2009; Redden et al., 2013; Shi et al., 2015a, b). The effects of the variation in the growth stages of the panicles and spikelets on seed-setting rates have often been overlooked or averaged in crop models (Bouman, 2001; Tang et al., 2009; Yoshida and Horie, 2009), which can be an important source of uncertainties.

Recently, new models have been developed which consider the flowering pattern in the field to estimate heat-induced spikelet sterility (Barlow et al., 2015; Nguyen et al., 2014; Shi et al., 2007). These models account for the distribution of the flowering events from a single panicle to the crop population, which is an important improvement in application to the field situation. However the sensitivity changes in the response of seed-setting to heat stress are not fully taken into account. Seed-setting involves a series of processes to complete in a short period, including dehiscence of anther, pollen shedding, germination of pollen grains and elongation of pollen tubes, which are susceptible to heat stresses (Mackill et al., 1982; Matsui et al., 2000; Prasad et al., 2006). The effects of heat events at different growth stages should therfore be better quantified.

One of the major bottlenecks in modeling seed-setting under heat stress is lack of the high quality experimental datasets. Most of the previous controlled experiments were conducted in chambers, which usually specified panicles at specific timing to single out factors (Matsui et al., 1997; Matsui et al., 2001; Satake and Yoshida, 1978), leading to the variations among different flowers often been overlooked and the crop-level responses of seed-setting to heat stress difficult to test. During 2011–2012 and 2014–2015, we initiated a series of high quality experiments in the chambers to determine the effects of short-term heat stress at different growth stages on seed-setting rates of the whole plants. This study was conducted (i) to quantify the heat stress by taking account into the interaction of high temperature intensites and durations, and (ii) to develop a model that can quantify the variation of seed-setting rates of the whole plants under the heat events at different stages from flowering stage.

2. Materials and methods

2.1. Experimental design

Dataset were obtained from the environment-controlled phytotrons experiments conducted in Nanjing (118.78°E, 32.04°N) from 2011 to 2012 and in Rugao (120.33°E, 32.23°N) from 2014 to 2015 in Jiangsu Province of China. The experimental methods and details are described fully by Shi et al. (2016). Briefly, three japonica rice cultivars, Nanjing41 (grown in 2011, 2012, 2014 and 2015), Wuxiangjing14 (grown in 2011 and 2012) and Wuyunjing 24 (grown in 2014 and 2015) were used in the experiments. Seeds of these cultivars are sown in nearby field and raised on the dry seedbed. Three-leaf seedlings were transplanted into plastic pots (height = 35.6 cm, inner diameter = 29.8 cm, volume 25.0 L filled with a soil of 22.5 L) and kept submerged until one week before harvest. The pots were placed closely together at a density of about 11 pots per m^2 and the transplanting density was two plants per hill and three hills per pot, equivalent to 66 plants per m^2, which is similar to a typical density in farmers' practice for japonica rice cultivars in the region of 60 to 75 plants per m^2 (Jiangsu Province Commission of Agricultural, 2011). 1.5 g N, 1.5 g P_2O_5 and 2 g K_2O were applied in each pot as basal fertilizer before transplanting, and the additional 0.3 g N and 1.2 g N were top-dressed at mid-tillering and panicle initiation, respectively. Irrigation, weed, and disease and pest control were carried out according to local standards of rice cultivation to avoid biotic and abiotic stresses.

The rice plants were grown under ambient condition before the heat stress treatments. We recorded the date when the first spikelet flowered on each panicle and determined the flowering date as 50% of panicles initiated flowering for each pot. Once the rice plants reached the target development stages of 0, 6 and 12 days after flowering (DAF), pots with plants of similar number of panicles and growth stage were transferred into each phytotron room (L × W × H; 3.4 m × 3.2 m × 2.8 m) for the designated treatments. Because there were about 4000 spikelets in a pot, the timings of flowering varied greatly. This resulted that the heat stress was imposed on spikelets of different growth stages including both pre-flowering and post-flowering depending on the positions of the panicles.

After the heat stress treatments were completed, the plants were moved out and grown outside until harvest. The heat stress treatments varied slightly from year to year, but four temperature regimes were set for all years; target daily maximum and minimum temperatures (T_{max}/T_{min}) were 32 °C/22 °C, 35 °C/25 °C, 38 °C/28 °C and 41 °C/31 °C in 2011 and 2012; 32 °C/22 °C, 36 °C/26 °C, 40 °C/30 °C and 44 °C/34 °C in 2014 and 2015. Durations were 2, 4 and 6 days in 2014 and 2015; 3, 5 and 7 days in 2011; 3, 6 and 9 days in 2012, which are summarized in Table 1. Air temperature (Ta, °C) and relative humidity (RH, %), soil volumetric water content (VWC, $m^3\ m^{-3}$) and photosynthetically active

Table 1
Summary of heat stress treatments in the environment-controlled phytotrons.

Year	Site	Cultivar	Sowing date	The timing of treatment[a]	Temperature level & duration[b]
2011	Nanjing	Nanjing 41 Wuxiangjing 14	5/25 5/18	12DAF	[T1, T3] × [D2] [T2, T4] × [D1, D2, D3]
2012	Nanjing	Nanjing 41 Wuxiangjing 14	5/23 5/23	12DAF	[T1,T2] × [D2*] [T3, T4] × [D1*, D2*, D3*]
2014	Rugao	Nanjing41 Wuyunjing 24	5/15 5/15	0 DAF & 6 DAF	[T1] × [D2**] [T2*, T3*, T4*] × [D1, D2, D3]
2015	Rugao	Nanjing41 Wuyunjing 24	5/12 5/17	0 DAF & 6 DAF	[T1] × [D2**] [T2*, T3*, T4*] × [D1**, D2**, D3**]

[a] 0 DAF: 0 day after flowering, 6 DAF: 6 days after flowering, 12 DAF: 12 days after flowering.
[b] T1, T2, T3, T4, T2*, T3* and T4* indicate the temperature levels (Tmax/Tmin) of 32/22 °C, 35/25 °C, 38/28 °C, 41/31 °C, 36/26 °C, 40/30 °C and 44/34 °C, respectively. D1, D2, D3, D1*, D2*, D3*, D1**, D2** and D3** indicate the durations of 3 days (d), 5 d, 7d, 3 d, 6 d, 9 d, 2 d, 4 d and 6 d under different temperature intensities, respectively.

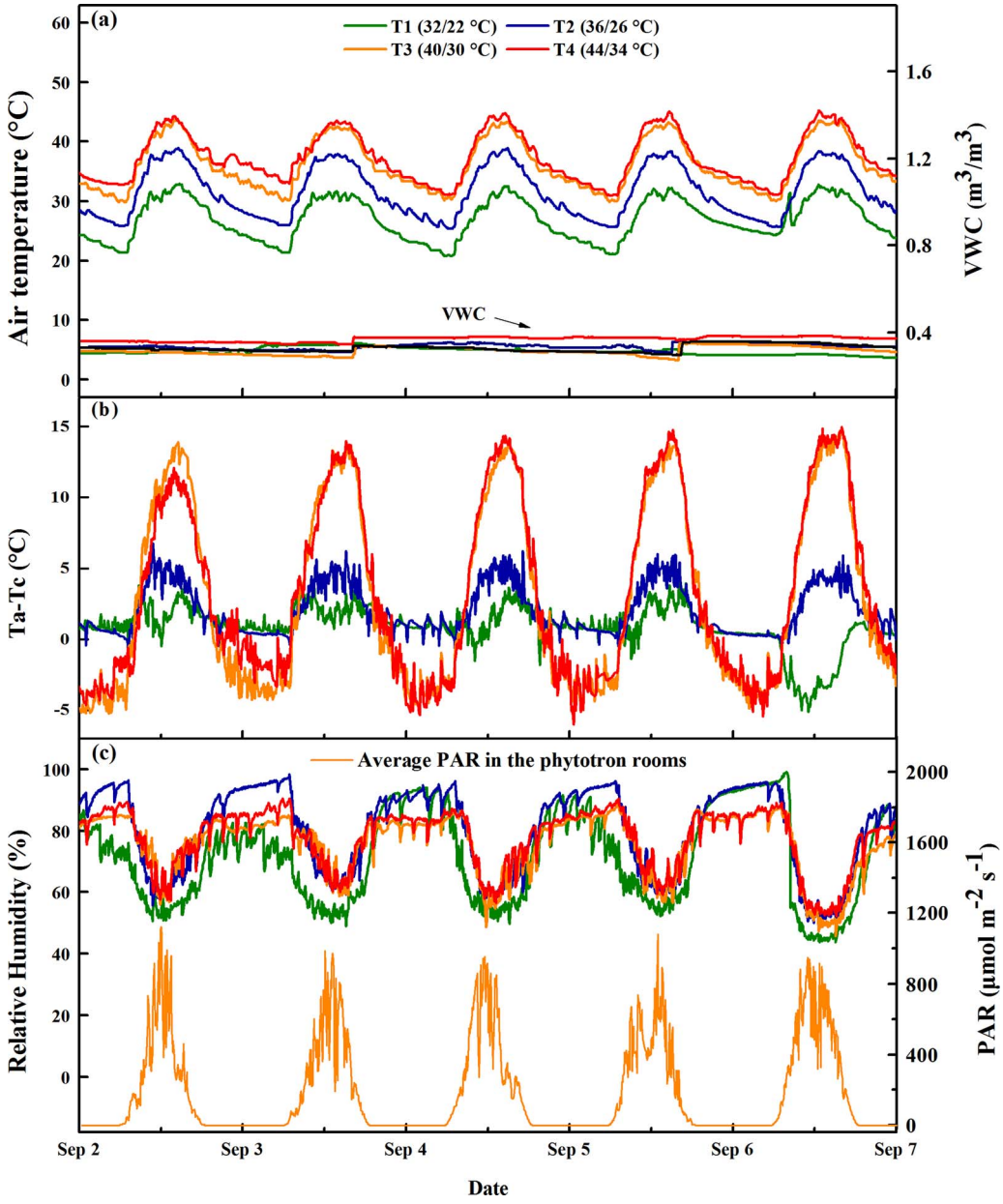

Fig. 1. Diurnal variations of air temperature (Ta, °C, a-left vertical axis), soil volumetric water content (VWC, $m^3\,m^{-3}$, a-right vertical axis), the difference between air temperature and plant surface temperature (Ta-Tc, °C, b-left vertical axis), relative air humidity (RH, %, c-left vertical axis) and average photosynthetically active radiation (PAR, $\mu mol\,m^{-2}\,s^{-1}$, c-right vertical axis) in phytotrons during heat stress treatments in 2014.

Table 2
Micrometeorological data during 6-day treatment periods starting from 0 DAF and 6 DAF in 2014 and 2015.

Micrometeorological variable[a]	Year	The starting time of treatment[b]	Average daily maximum[c]				Average daily minimum			
			T1	T2	T3	T4	T1	T2	T3	T4
Ta (°C)	2014	0 DAF	32.3	38.3	43.1	44.4	21.1	25.6	30.0	31.7
		6 DAF	32.7	37.3	39.4	43.7	22.1	26.5	30.1	33.6
	2015	0 DAF	31.5	35.9	39.8	43.4	20.7	26.3	26.7	31.1
		6 DAF	31.1	35.8	40.9	44.4	20.7	26.5	27.0	31.2
	Average		31.9	36.8	40.8	44.0	21.2	26.2	28.4	31.9
Tc (°C)	2014	0 DAF	30.3	34.5	37.5	38.6	19.9	25.1	28.8	29.8
		6 DAF	31.7	36.1	36.4	40.2	21.5	25.0	28.4	31.6
	2015	0 DAF	29.4	32.4	35.0	38.3	19.7	24.5	25.8	29.6
		6 DAF	29.4	32.6	36.7	39.6	19.7	24.6	25.4	29.1
	Average		30.2	33.9	36.4	39.2	20.2	24.8	27.1	30.0
Ta-Tc (°C)	2014	0 DAF	3.2	5.5	13.6	13.9	−0.6	−0.4	−4.8	−4.8
		6 DAF	3.0	5.3	12.5	12.5	−0.3	−1.1	−5.2	−5.1
	2015	0 DAF	4.1	4.4	7.8	7.5	−1.2	0.2	−0.8	0.3
		6 DAF	4.7	4.2	9.9	10.6	−1.6	−0.3	−0.2	0.6
	Average		3.7	4.9	10.9	11.1	−0.9	−0.4	−2.7	−2.3
RH(%)	2014	0 DAF	91.6	96.0	89.1	86.7	50.4	54.6	56.0	52.2
		6 DAF	69.9	77.9	79.4	75.5	39.6	50.2	60.8	55.3
	2015	0 DAF	90.2	88.3	94.7	90.3	63.4	62.9	61.3	62.5
		6 DAF	76.4	74.5	80.4	86.5	48.7	50.6	49.6	58.7
	Average		82.0	84.2	85.9	84.8	50.5	54.6	56.9	57.2
VPD (hPa)	2014	0 DAF	23.0	29.6	37.0	42.7	2.6	1.3	4.7	6.3
		6 DAF	20.5	23.4	21.6	28.8	2.6	7.5	8.0	11.4
	2015	0 DAF	13.4	19.7	20.3	24.6	2.7	8.4	2.3	5.2
		6 DAF	21.1	27.4	38.0	37.7	6.8	8.4	7.3	7.0
	Average		19.5	25.0	29.2	33.5	3.7	6.4	5.6	7.5

[a] Ta and Tc indicate air temperature (°C) and plant surface temperature (°C), respectively; RH indicates relative humidity (%); VPD indicates vapor pressure deficit (hPa).
[b] 0 DAF: 0 day after flowering, 6 DAF: 6 days after flowering.
[c] T1, T2, T3 and T4 indicate the temperature levels (Tmax/Tmin) of 32/22 °C, 36/26 °C, 40/30 °C and 44/34 °C, respectively.

radiation (PAR, μmol $m^{-2} s^{-1}$) in the phytotrons were measured with VP-3 sensor (Decagon Devices, Pullman, Wash, USA), 5TM sensor (Decagon Devices, Pullman, Wash, USA) and PYR solar radiation sensor (Decagon Devices, Pullman, Wash, USA), respectively. Temperature and relative humidity in the phytotrons were controlled to simulate the pattern of local ambient environment with the target set every hour. Ta, Tc, RH, VWC and PAR were continuously recorded as shown in Fig. 1. VPD was calculated according to the Guide to Meteorological Instruments and Methods of Observation (WMO). For 0 and 6 DAF treatments in 2014 and 2015, plant surface temperature (Tc, °C) was also monitored with the infrared radiometer (SI-111, Apogee Instruments, Logan, Utah, USA) placed at 1.6 m above ground and facing diagonally downward toward the plant surface for an area of 0.8 m^2 at the center of the chamber.

Averaged across the seasons, measured maximum Ta was within 0.1–0.8 °C from the target, but minimum Ta was generally lower than the target by as much as 2.1 °C. Minimum (or daytime) RH ranged from 51 to 57%, which was similar to the ambient in Jiangsu, China. VPD ranged from 19.5 to 34 hPa, being greater in higher temperature treatments. Tc was generally lower than Ta, and the Ta-Tc difference became larger as the temperatures increased. In T4, Ta-Tc difference was 11.1 °C during the daytime.

During the treatment, 10 panicles in each treatment likely to flower soon were marked and digital photos of the panicles were taken every two hours from 8:00 to 16:00 to observe the time of flowering until all the spikelets on the marked panicles finished flowering. The photos were taken from the same side, so the spikelets on the blind side could not be seen. We therefore counted newly-opened spikelets on one side and estimated a total number by doubling it. The primary rachis branches in each panicle were grouped into three parts according to their vertical positions on the panicle, namely the upper, middle and lower panicles. Frequency of timing of flowering on each part of the panicles was recorded. At physiological maturity, 5-pot plants were harvested for each treatment. As with the previous observation of flowering, panicles were divided into three parts. Sterile grains and fertile grains were identified manually by pressing spikelets between thumb and index finger. The seed-setting rate was calculated as the ratio of the number of fertile spikelets to the total number of spikelets.

2.2. Model description

To analyze the changes of rice in sensitivity to heat stress with different timings, four different heat stress indices (*HSI*), i.e., maximum, minimum and mean air temperature averaged for the treatment periods (T_{max}, T_{min} and T_{mean}, °C), and heating degree-day (HDD, °C d) were tested in this research. Seed-setting rates were fitted to a logistic function with *HSI*, as shown in the following equation:

$$SR(HSI) = \frac{SR_{max}}{1 + \exp\{b(HSI - c)\}} \quad (1)$$

where *SR* is the seed-setting rate (%); *HSI* is the heat stress index, which can be represented with the maximum, minimum and mean air temperatures averaged for the treatment periods, and HDD during the treatment periods; SR_{max} is the potential seed-setting rate. Parameter b represents the slope near the knee point of the logistic curve. Parameter c is the heat stress index at the inflexion point that reaches 50% of SR_{max}.

Heating degree-day (HDD), defines as the cumulative temperature above a critical value, was applied to account for the combined effects of heat stress intensity and duration according to Shi et al. (2015a, b), which was calculated using the following equations:

$$\mathrm{HDD} = \sum_{d_h}^{d_m} HD_i \quad (2)$$

$$HD_i = \frac{1}{24} \sum_{j=1}^{24} \mathrm{Max}(T_j - \tau, 0) \quad (j = 1, 2, ..., 24) \quad (3)$$

where d_h and d_m are the dates of heading and maturity, HD_i is the heating degree-day of day i, T_j is the hourly air temperature calculated as the mean of the 12 records per hour, and τ is the temperature

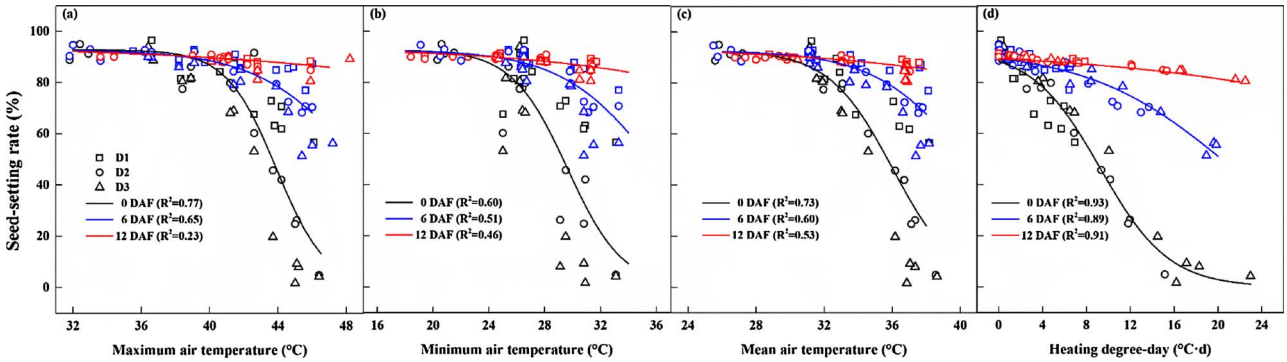

Fig. 2. Observed and fitting seed-setting rates (%) in relation to maximum air temperature (a), minimum air temperature (b), mean air temperature (c) and heating degree-day (d, τ = 35 °C). D1, D2, and D3 indicate heat treatments for 2, 4 and 6 days, respectively. 0 DAF, 6 DAF and 12 DAF indicate the timing of treatments, which are 0, 6 and 12 days after flowering, respectively. The data used in the graph were observed from the 0 DAF, 6 DAF and 12 DAF treatments.

threshold of heat stress.

As development of each spikelet varied among panicles and even among those on the same panicle, variation in the spikelet flowering time was apparent among upper, middle and lower parts of the panicle. Therefore, the lags of flowering stage for the spikelets on the upper, middle and lower panicles were defined as Δwu, Δwm and Δwl, respectively, compared to the whole panicles, which are summarized in Table 2.

We tested whether the response of seed-setting rates to temperatures changes depending on the different treatment periods or on the vertical positions on the panicles, by examining stage dependence of the parameters of Eq. (1). To incorporate the stage-dependent parameters into Eq. (1), we expressed the seed-setting rate of rice population (SR, %) at maturity as a function of potential seed-setting rate and a reduction factor (Sterility) by the daily heat stress index (HSI_i);

$$SR = SR_{max} - Min\left(\sum_{d_h}^{d_m} Sterility(HSI_i),\ SR_{max}\right) \quad (4)$$

$$Sterility(HSI_i) = SR_{\max} - SR(HSI_i) \quad (5)$$

where d_h and d_m are the dates of heading and maturity, HSI_i is the heat stress index of day i during heading and maturity. $Sterility(HSI_i)$ is the sterility rate (%) of day i, $SR(HSI_i)$ is the actual seed-setting rate (%) of day i calculated by Eq. (1), SR_{max} is the cultivar-specific potential seed-setting rate (%). For Eqs. (4) and (5), we used the maximum seed-setting rate in the observations for each cultivar as SR_{max}. We also compared model performance between with and without stage-dependent response in Eq. (4).

2.3. Parameter estimation and evaluation

A resampling method of bootstrap (Efron and Tibshirani, 1993) was used to select datasets for parameter estimation and evaluation to test whether our model is suitable for predicting the seed-setting rate in response to the heat stress from the flowering stage. If the size of the dataset is n, a bootstrap sample can be created by sampling n instances uniformly from the original data. Since the data is sampled with replacement, the probability of any given instance not being chosen after n samples is $(1-1/n)^n$ (Kohavi, 1995). Here n was equal to 112, the total number of treatments in our datasets. Therefore, we randomly sampled about 63% of the datasets to constitute a training set and the rest (about 37%) was used as a testing set. Optimal parameters that minimize the mean square errors were selected using the training set, and the parameter set was applied to the testing set and root mean square error (RMSE) and mean bias error (MBE) were calculated. We repeated these steps for 1000 times to estimate variation in the parameters. Median values of 1000 times optimal parameters were used to represent the final parameter values. MATLAB (Version 8.2, MathWorks, Inc.) was used for all procedures including re-sampling, parameter estimation and cross-validation.

2.4. Sensitivity analysis

To test the sensitivity of seed-setting rate to different timing and intensity of heat stress in our model, we simulated the seed-setting rates under a series of heat stress scenarios, where heat stress occurred from 0 DAF to 25 DAF, and at each timing the temperature intensities ranged from 35 °C to 45 °C at 0.1 °C intervals with a duration of 4 days. In this simulation, we assumed that the difference between daily maximum air temperature and minimum air temperature was 10 °C, and that the hourly temperatures (T_j) could be approximated by the following cosine curve:

$$T_j = \frac{T_{max} + T_{min}}{2} + \frac{T_{max} - T_{min}}{2} * cos\left(\frac{j-14}{12}\pi\right) \quad (6)$$

where T_{max} and T_{min} are the daily maximum air temperature and minimum air temperature, respectively, T_j is the hourly air temperature estimated from T_{max} and T_{min}.

3. Results

3.1. Comparison among heat stress indices

Seed-setting rates of the whole panicles were fitted to a logistic function of four heat stress indices (HSI) as T_{max}, T_{min}, T_{mean} and HDD (Eq. (1)) with the training dataset (Fig. 2). The temperature threshold for HDD (τ) was set at 35 °C according to the previous studies (Horie, 1993; Satake and Yoshida, 1978; Shi et al., 2016). The logistic function with all four HSIs provided a significant fit to the data, but the coefficient of determination (R^2) ranged from 0.23 to 0.92. Within four HSIs, HDD was the most appropriate explanatory variable to describe the effects of heat stress on seed-setting.

In order to test whether there was a variety difference in τ, we studied the fitness and parameters of the logistic function of HDD in response to the step-wise change in the threshold from 30 °C to 40 °C at every 0.5 °C interval. The logistic curve fitted best when the thresholds of HDD were set to 35 °C, 36 °C, 35.5 °C respectively for Nanjing 41, Wuxiangjing14 and Wuyunjing 24, nonetheless, the R^2 corresponding to different τ were mostly higher than 0.9 (Data not shown).

Similarly, we tested whether τ changes with growth stages of 0 DAF, 6 DAF and 12 DAF. The box-plot showed the variations of the parameter b, parameter c and R^2 of the logistic curves in response to τ (Fig. 3). Each parameter showed distinct changes depending on the timing of heat stress (Fig. 3). When τ was increased, parameter c decreased but b increased. At 0 DAF, the change in parameter b in response to τ was greater than that in parameter c, but vice versa at 12

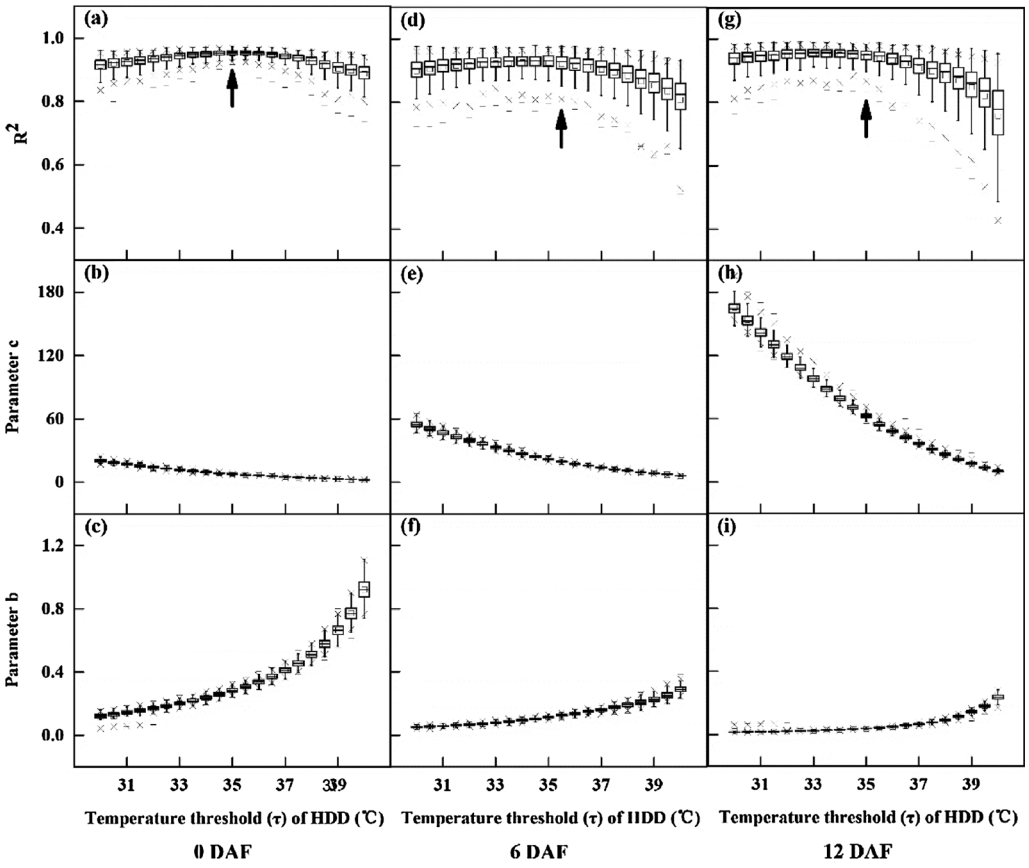

Fig. 3. Parameter b (c, f, i), parameter c (b, e, h) and determination coefficient (a, d, g) of logistic curves to fit seed-setting rates (%) with heating degree-day (HDD) above diverse thresholds of heat stress occurred separately at 0 (a, b, c), 6 (d, e, f) and 12 days (g, h, i) after flowering. Variation of the parameters was estimated based on the 1000-group training datasets with the bootstrap resampling methods. The maximum value, 75th percentile, 50th percentile (median), mean (optional), 25th percentile, minimum value and outlier were shown from top to bottom in the box-plot. All the varieties were used in the graph.

DAF, while both parameters changed moderately at 6 DAF. On the other hand, τ that showed the maximum R^2 was similar at 35 °C, 35.5 °C and 35 °C, respectively, for treatments at 0, 6 and 12 DAF.

3.2. Seed-setting rates at different positions of the panicles in response to HDD

Seed-setting rates at different positions of panicles in response to heat stress at different stages were fitted well to a logistic function of heating degree-day (HDD), as shown in Fig. 4. The positions included upper, middle and lower parts of the panicle, and the timing of treatments were 0, 6 and 12 DAF, respectively. Heat stress at flowering dramatically decreased the seed-setting rates. When HDD exceeded 20 °C d, all spikelets were empty. Sterility was much less when heat was imposed at 6 DAF relative to that at 0 DAF, and that at 12 DAF was more moderate. At 0 DAF, seed-setting rates of upper panicles were most sensitive to heat stress, followed by the middle and lower ones. However, for the treatment periods of 6 DAF or 12 DAF, seed-setting rates of lower panicles were most sensitive to heat stress, then middle ones, then upper ones.

3.3. Flowering distribution of spikelets on different positions of the panicles

We observed that flowering of spikelets on the upper panicles peaked around 3 DAF, while that of middle and lower panicles delayed around 1 and 2.5 days, respectively (Fig. 5). The cumulative frequency

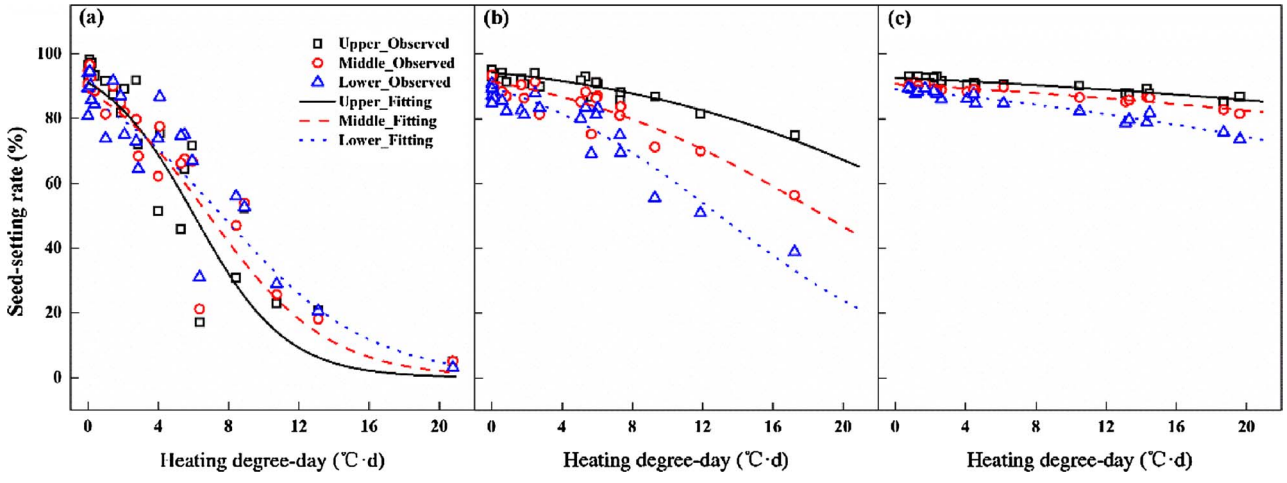

Fig. 4. Observed and fitted seed-setting rates (%) of upper, middle and lower parts of the panicles in relation to heating degree-day (HDD) at treatment periods of 0 (a), 6 (b) and 12 (c) days after flowering. All the varieties were used in the graph (τ was set to 35 °C, 36 °C, 35.5 °C respectively for Nanjing 41, Wuxiangjing14 and Wuyunjing 24).

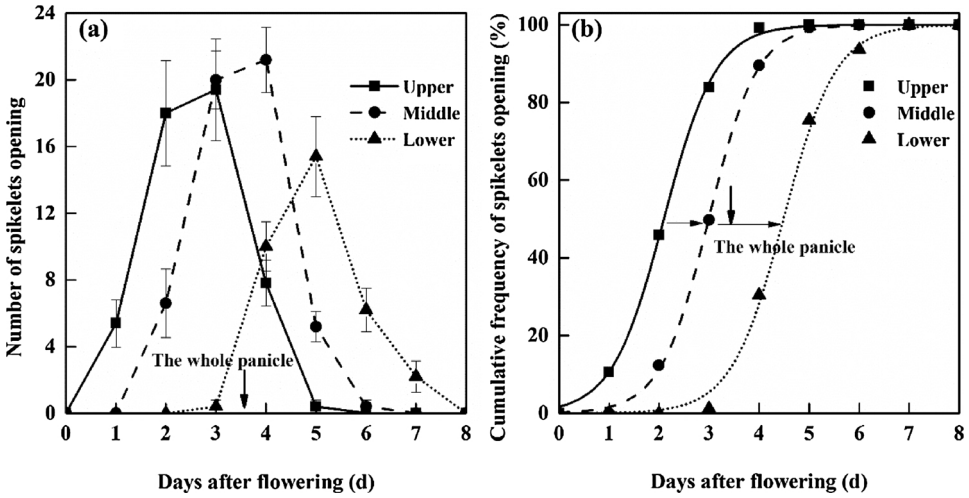

Fig. 5. Number of spikelets opening on the upper, middle and lower parts of the panicles (a) and cumulative frequency of spikelets opening (b) in relation to days after flowering. The vertical arrows indicate the average date of flowering for the whole panicles.

of florets opening clearly indicated 1 and 3-day delay of flowering for the spikelets on the middle and lower parts of the panicles, respectively, compared to the upper panicles. The date of flowering averaged for the whole panicles was 1.5 days later than that of spikelets on the upper panicles. Thus, Δwu, Δwm, and Δwl (Table 2) were assigned the values of 1.5, 0.5 and −1.5 days.

3.4. Parameters in response to the timing of the treatments

When we used HDD to quantify the effects of heat stress on seed-setting rates, we found that parameter b and c were highly correlated (Fig. 7a) and that the product of them was approximately 3. We therefore simplified Eq. (1) when we used HDD as an HSI:

$$SR(HSI) = \frac{SR_{max}}{1 + \exp(b * \mathrm{HDD} - 3)} \quad (7)$$

Where SR is the seed-setting rate (%), SR_{max} is the potential seed-setting rate. HDD is the heating degree-day (°C d). Parameter b determines the shape of logistic curve.

Parameter b changed largely with the stages of the treatments and positions of panicles, which could be expressed as a curve in relative to the timing of treatments (Fig. 6). Here, the flowering stage of the whole panicle was used as a reference date (0). Differences in flowering of the spikelets on the upper, middle and lower parts of the panicles are accounted for by Δwu, Δwm, and Δwl (Table 3). Parameter b increased toward flowering and peaked around 2 DAF, but then onward decreased sharply till 10 DAF.

3.5. Model evaluation

The estimated parameters b was tested against the independent data that were not used for the parameterization. Two versions of the models were tested for Eqs. (4) and (5): one is the model with constant parameter b (0.18) (Model 1), and the other with stage-dependent parameters as shown in Fig. 6 (Model 2). The seed-setting rates exposed to heat stress predicted by Model 1 differed greatly from the observations at 0 and 6 DAF (Fig. 7a, R^2 = 0.28, RMSE (%) = 20.13). On the other hand, the seed-setting rates predicted with Model 2 showed good agreement with the observed values, and goodness of fit improved significantly to R^2 of 0.89 (Fig. 7b), in which the slope of regression lines did not differ significantly from 1.0 and the data scattered around the 1:1 line.

Furthermore, the performance of Model 2 was evaluated for each stage. Fig. 8 shows the variations of RMSE and MBE obtained with 1000 repetitions of bootstrap samples. At 0 DAF, RMSE was slightly greater compared to that at other stages, and MBE was positive, indicating that the model tends to overestimate the observed seed-setting rates. The goodness of fit improved significantly at 6 DAF and 12 DAF, although at 6 DAF, the model tended to underestimate as evidenced by negative MBE. Generally, the performance of Model 2 was much improved

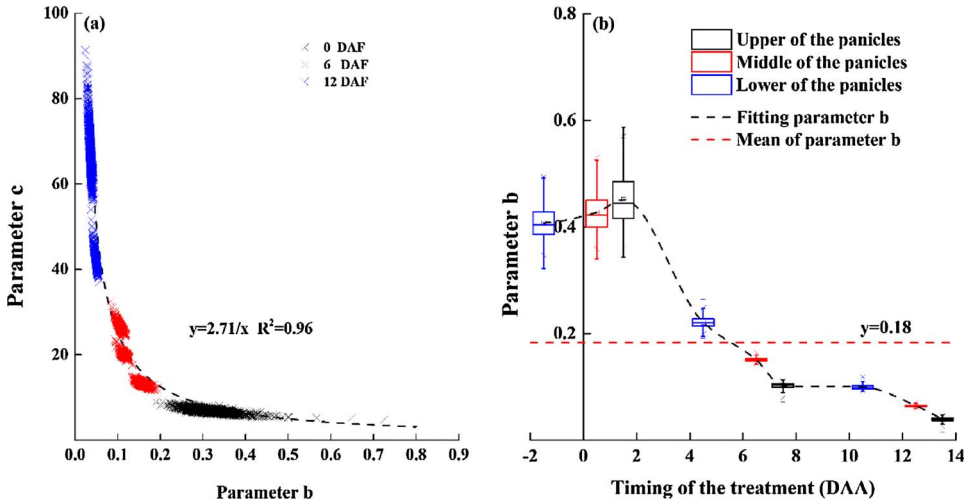

Fig. 6. Relationship between parameter b and c of logistic curves (a) in Eq. (1), and parameter b of logistic curves (b) in Eq. (7) in response to the timing of heat stress treatments. Variation of the parameters was estimated based on the 1000-group training datasets with the bootstrap resampling methods. The maximum value, 75th percentile, 50th percentile (median), mean (optional), 25th percentile, minimum value and outlier were shown from top to bottom in the box-plot.

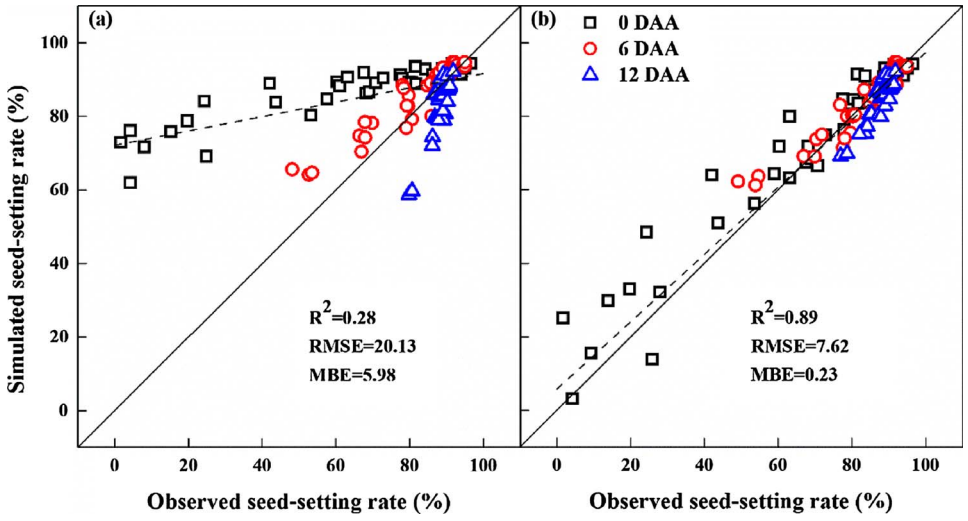

Fig. 7. Comparison between observed and simulated seed-setting rates (%) by Model 1 with constant parameters across different growth stages (a) and Model 2 with stage-dependent parameters (b). 0, 6 and 12 DAF are the treatments started at 0, 6 and 12 days after flowering. The simulated data in the graph was based on the median value of parameter sets estimated from 1000-group training datasets with the bootstrap resampling methods.

Table 3
Timing of heat stress treatments for spikelets on different positions of the panicles relative to the date of flowering of the whole panicle.

Position of panicle in rice population	Treatment period (days after flowering)		
The whole panicle	0	6	12
Upper panicle	0 + Δwu[a]	6 + Δwu	12 + Δwu
Middle panicle	0 + Δwm[b]	6 + Δwm	12 + Δwm
Lower panicle	0 + Δwl[c]	6 + Δwl	12 + Δwl

[a] Δwu.
[b] Δwm.
[c] Δwl: Delays of flowering stage (days) for the spikelets on the upper, middle and lower parts of the panicles compared to the average days after flowering for the whole panicles, respectively. Δwu, Δwm and Δwl were 1.5 d, 0.5 d and −1.5 d, respectively.

compared to Model 1, with significantly reduced RMSE (median = 7.62) and virtually no bias if three stages combined.

3.6. Sensitivity analysis

The effects of four-day heat stress of different intensities on relative seed-setting rate were examined for the period from 0 to 25 DAF (Fig. 9). The simulated response surface showed that seed-setting rates are most sensitive to high temperatures from 0 to 7 DAF, where temperatures higher than 42 °C reduce grain setting rate to less than half of SRmax. The sensitivity decreases sharply after 7 DAF but persists until 15–20 DAF. After 22 DAF heat stress had almost no effect on seed-setting rate (relative SR > 95% even under 45 °C).

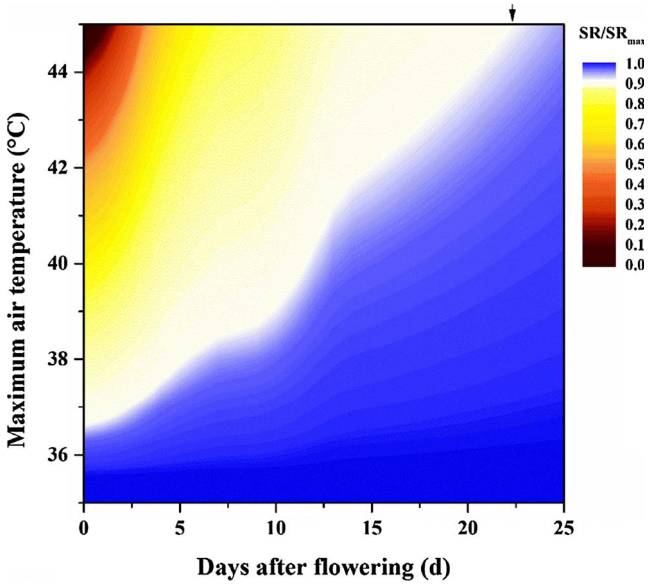

Fig. 9. Simulated effects of 4-day heat stress with different intensities and timings on seed-setting rate/potential seed-setting rate (SR/SRmax, Eq. (4)) for 25 days after flowering, using the model with the stage-dependent parameters. The difference between daily maximum air temperature and minimum air temperature is assumed to be 10 °C, and hourly temperatures are as approximated by a cosine curve (Eq. (6)) to calculate HDD.

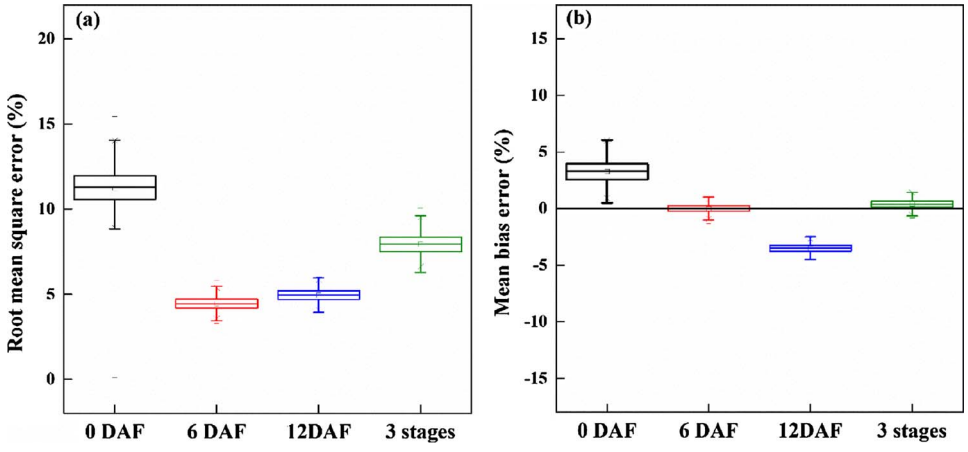

Fig. 8. Root mean square error (RMSE) (a) and mean bias error (MBE) (b) between observed and simulated seed-setting rates (%) by Model 2 (with stage-dependent parameters) under the heat stress occurred at the stages of 0 DAF, 6 DAF, 12 DAF, and the average performance under the heat stress treatments across all 3 stages. The simulated data was based on the median value of parameter sets estimated from 1000-group training datasets with the bootstrap resampling methods. Variation in the goodness of fit for 1000 independent tests was shown in the box-plot. The maximum value, 75th percentile, 50th percentile (median), mean (optional), 25th percentile, minimum value and outlier were shown from top to bottom in the box-plot.

4. Discussion

Extreme heat events become more frequent during the crop growing season with various intensities and durations. Models for simulating heat stress on crop seed-setting rates have often been developed based on the temperature controlled experiments with fixed duration of the heat stress treatments (Horie, 1993; Jagadish et al., 2007; Nguyen et al., 2014). These models, however, have rarely been tested against experimental datasets obtained under a range of intensities and durations of the heat events, because such datasets are not often available. In this study, we tested heat stress indices and models for quantifying heat stress effects on seed-setting rates in rice crop exposed to various intensities and durations of heat stress at different stages from flowering. We confirmed that logistic functions fitted well to these observations, but demonstrated gradual changes in the temperature sensitivity parameters over different grain growth stages from the heat treatments at 0, 6 and 12 DAF with the durations of 2, 4 and 6 days. These high-quality datasets allow us to examine the exact threshold value of heat stress, and to quantify the sensitivity of seed-setting rates to heat stress at different stages from flowering.

4.1. Heat stress index

We compared the fitting results of four different heat stress indices (Fig. 2), T_{max}, T_{min}, T_{mean} and HDD, and found that HDD was the best. All these four heat indices are often used to quantify the effects of heat stress in crop growth models (Bouman, 2001; Keating et al., 2003; Liu et al., 2016; Shi et al., 2015a, b; Tang et al., 2009). T_{max} and T_{mean} fitted better with seed-setting rates than T_{min}, showing that heat stress during daytime had a stronger effect on seed-setting rates than nighttime heat stress. This agreed with the previous observations that heat events during flowering period are influential (Jagadish et al., 2007) and that spikelet sterility was highly correlated with maximum temperature during flowering and not much with minimum temperature (Ishimaru et al., 2016). However, the seed-setting rates varied greatly even at the same T_{max} and T_{mean} (Fig. 2), indicating temperature intensity alone is not sufficient to give reliable estimates. Instead, HDD, a cumulative heat dose, accounting for both intensity and duration of heat events, could better explain the variation of heat stresses on the seed-setting rates, confirming the previous observations in the chamber (Jagadish et al., 2007) and in the open field (Hasegawa et al., 2011). This indicates that the effect of heat above the critical temperatures during grain growth is irreversible (Wahid et al., 2007), even cooler weather after the heat events does not offset the negative effects of heat stresses. For these reasons, we conclude that HDD provides a reliable basis to quantify the effects of heat stress on seed-setting rate.

4.2. Temperature thresholds of HDD

Previous researches showed that the threshold (τ) of HDD for seed-setting does exist (Sánchez et al., 2014), but it remains unclear whether it varies with growth stages. In this study, we examined τ for 0 DAF, 6 DAF and 12 DAF treatments by fitting a logistic function of HDD with variable τ to the seed-setting rates. Overall, τ is not a strongly sensitive parameter for overall fit, but was similar among the treatments at 0 DAF, 6 DAF and 12 DAF (Fig. 3), ranging from 35.0 °C to 35.5 °C. We conclude that the high temperature threshold of HDD could be treated as a fixed parameter over the period from flowering onward for a specific variety.

A large genotypic difference has been reported for the heat stresses (Jagadish et al., 2007; Matsui et al., 2001; Satake and Yoshida, 1978; Yoshida, 1981), and τ can differ among cultivars (Maruyama et al., 2013). In the present study, however, τ of the three varieties tested in our study was similar, if a difference of 0.5–1 °C could be tolerated: 35 °C, 36 °C and 35.5 °C for Nanjing 41, Wuxiangjing14, and Wuyunjing 24, respectively. The three varieties were reported to have different heat tolerances according to previous studies (Shi et al., 2016; Zhang et al., 2007; Zheng et al., 2004) and Chinese Crop Germplasm Resources Information System (CGRIS), but we could not confirm the apparent differences in τ among the varieties tested. The variation of the parameter τ among cultivars of contrasting heat tolerance needs to be tested in future studies.

4.3. Temperature sensitivity at different growth stages

Stage sensitivity to heat stress has been found in a variety of crops (Erickson and Markhart, 2002; Gross and Kigel, 1994; Guilioni et al., 1997; Prasad et al., 2008; Shi et al., 2016; Wahid et al., 2007). Likewise, in this study, the logistic parameters b and c changed greatly with the timing of the heat events (Fig. 4.), which reflected the variation of physiological sensitivity to heat stress at different growth stages. The sensitivity to heat stress was greatest at around anthesis and decreased from then onward, which agreed with the previous findings by Satake and Yoshida (1978) and Yoshida (1981). Compared to their studies in which spikelet fertility of the main culm was studied, this study showed a slower change in sensitivity over time, in other words, the effects persisted over the longer period after anthesis.

The change of sensitivity can be partly attributed to the flowering pattern among the rice population. The distribution of heading dates in a field is often unsymmetric and follows the Poisson probability distribution function. Anthesis of spikelets varied even in the same panicle and followed a normal distribution function (Nguyen et al., 2014), as shown in Fig. 5. Spikelets on the upper branches of the panicle flowered first, then those on the middle, and finally at the base (Tanaka et al., 2014). A combination of the distribution of heading dates in the field and the distribution of flowering time in the panicle results in a flowering pattern that peaks at the early anthesis stage and takes about 15–20 days for all the spikelets to complete anthesis in the field (Yoshida, 1981).

However, seed-setting rate is not just a result of flowering and pollination, which complete just within about 1–2.5 h (Yoshida, 1981). There is approximately a 5-days window between panicle emergence and onset of grain filling (Morita et al., 2005; Zhang et al., 2013). Even after flowering, there is still a direct influence of heat stress on the seed-setting rates. Heat-induced abortion has been reported in pea where growing pods compete with the youngest reproductive organs (Guilioni et al., 1997). Similarly, the superior and inferior spikelets of rice could often compete for carbohydrate and nitrogen during grain filling (Ting et al., 2015), meanwhile heat stress can accelerate grain growth (Morita et al., 2005) and thus demand for carbon and nitrogen, and thereby intensify the competition. This means there are possibilities that heat stress can reduce seed-setting, even after flowering, which can result in a gradual change in temperature sensitivity (Fig. 9) overlooked by previous models.

4.4. Remaining challenges

This work was conducted in the phytotron to ensure accurate control of temperatures and other environmental factors. Recent studies, however, suggested that temperature functions obtained in the chamber can be different under the field conditions, largely because of the gaps between air and crop or panicle temperatures, particularly in extremely hot and dry climate, where high transpirational cooling reduces the canopy temperature compared to air (Julia and Dingkuhn, 2013; Matsui et al., 2014), suggesting that vapor pressure deficit (VPD) or relative humidity are also important determinants for seed-setting rates. Projections of relative humidity under climate change, however, are highly uncertain. As indicated by Sherwood et al. (2010), relative humidity will remain almost constant under global warming if there is ample water on the surface. Assuming the lowland paddy ecosystems, where field is kept flooded, it is possible that relative humidity will not change much even when temperatures rose, which could be quite alarming. We

therefore attempted to control relative humidity at a similar level among different treatments. Observed daily minimum (daytime) RH ranged from 50 to 60% (Table 2), which resulted in a greater VPD in the higher temperature treatment (19.5 hPa in T1 and 34 hPa in T4). As a result, plant surface temperature (Tc) was lower than Ta and the Ta-Tc difference in the daytime ranged from 3.7 to 11.1 °C, being greater as Ta increased (Table 2). Because we did not measured Tc in all years throughout the growing period, we used Ta as an explanatory variable, but our results need to be coupled with a submodule for estimating crop or panicle temperatures such as Yoshimoto et al. (2011)'s model before this can be applied to actual field conditions.

Our quantitative study of heat-induced sterility and stage sensitivity allows us to simulate the effects of diverse heat events during the period from flowering onward on seed-setting rates, but other processes of rice growth and yield formation are still not evaluated, such as the assimilate accumulation and partitioning to different organs, grain weight. Uncertainties associated with heat stress in crop models remain largely unquantified, thus it is an effort to test and improve the crop models with experiment data in the next step.

5. Conclusions

Heat waves can have detrimental effects on rice yield has been reported, while quantifying the heat-sensitive processes for seed-setting rate is still difficult because so many parameters are involved. In this study, we proposed a simple model which can be used to estimate the final seed-setting rates under different heat stress durations and intensities by using the logistic function of HDD with the stage-dependent parameters. Because these parameters and functions were obtained from widely different temperature ranges imposed at different growth stages, the proposed model can be a basis for predicting rice yield under climates with frequent heat events. The validity of the model needs to be evaluated under the field conditions, by incorporating this into crop growth models.

Acknowledgements

This work was supported by the National Key Research and Development Program of China (2016YFD0300110), the National Science Foundation for Distinguished Young Scholars (31725020), the National Science Foundation of China (31571566), the Natural Science Foundation of Jiangsu province (BK20151435), the 111 Project (B16026), the Priority Academic Program Development of Jiangsu Higher Education Institutions (PAPD), and the China Scholarship Council (CSC).

References

Aggarwal, P.K., Mall, R.K., 2002. Climate change and rice yields in diverse agro-environments of India. II. Effect of uncertainties in scenarios and crop models on impact assessment. Clim. Change 52 (3), 331–343.

Asseng, S., Ewert, F., Rosenzweig, C., Jones, J., Hatfield, J., Ruane, A., Boote, K.J., Thorburn, P.J., Rötter, R.P., Cammarano, D., 2013. Uncertainty in simulating wheat yields under climate change. Nat. Clim. Change 3 (9), 827–832.

Barlow, K.M., Christy, B.P., O'Leary, G.J., Riffkin, P.A., Nuttall, J.G., 2015. Simulating the impact of extreme heat and frost events on wheat crop production: a review. Field Crop Res 171 (Suppl. C), 109–119.

Bouman, B., 2001. ORYZA2000: Modeling Lowland Rice, 1. IRRI.CGRIS. Chinese Crop Germplasm Resources Information System. http://www.cgris.net/cgris_english.html.

Efron, B., Tibshirani, R.J., 1993. An Introduction to the Bootstrap. Number 57 in Monographs on Statistics and Applied Probability. Chapman & Hall, New York.

Erickson, A., Markhart, A., 2002. Flower developmental stage and organ sensitivity of bell pepper (Capsicum annuum L.) to elevated temperature. Plant Cell Environ. 25 (1), 123–130.

Gross, Y., Kigel, J., 1994. Differential sensitivity to high temperature of stages in the reproductive development of common bean (Phaseolus vulgaris L.). Field Crop Res. 36 (3), 201–212.

Guilioni, L., Wery, J., Tardieu, F., 1997. Heat stress-induced abortion of buds and flowers in pea: is sensitivity linked to organ age or to relations between reproductive organs? Ann. Bot. 80 (2), 159–168.

Hasegawa, T., Ishimaru, T., Kondo, M., Kuwagata, T., Yoshimoto, M., Fukuoka, M., 2011. Spikelet sterility of rice observed in the record hot summer of 2007 and the factors associated with its variation. J Agric. Meteorol. 67 (4), 225–232.

Hasegawa, T., Kuwagata, T., Nishimori, M., Ishigooka, Y., Murakami, M., Yoshimoto, M., Kondo, M., Ishimaru, T., Sawano, S., Masaki, Y., 2009. Recent Warming Trends and Rice Growth and Yield in Japan, MARCO Symposium on Crop Production Under Heat Stress: Monitoring, Impact Assessment and Adaptation. National Institute for Agro-Environmental Studies, Tsukuba, Japan.

Horie, T., 1993. Predicting the effects of climatic variation and elevated CO2 on rice yield in Japan. J. Agric. Meteorol. 48 (5), 567–574.

Horie, T., Matsui, T., Nakagawa, H., Omasa, K., 1996. Effects of elevated CO2 and global climate change on rice yield in Japan. Climate Change and Plants in East Asia. Springer, pp. 39–56.

IPCC, 2013. Working group I contribution to the IPCC fifth assessment report cli- mate change 2013. The Physical Science Basis, Summary for Policymakers. . www.climatechange2013.org/images/uploads/WGIAR5-SPM_Approved27Sep2013.pdf.

Ishimaru, T., Xaiyalath, S., Nallathambi, J., Sathishraj, R., Yoshimoto, M., Phoudalay, L., Samson, B., Hasegawa, T., Hayashi, K., Arumugam, G., 2016. Quantifying rice spikelet sterility in potential heat-vulnerable regions: field surveys in Laos and southern India. Field Crop Res. 190, 3–9.

Jagadish, S.V., Craufurd, P.Q., Wheeler, T.R., 2007. High temperature stress and spikelet fertility in rice (Oryza sativa L.). J. Exp. Bot. 58 (7), 1627–1635.

Jiangsu Province Commission of Agricultural, 2011. Technical Specification for Rice Seedling. http://www.jsagri.gov.cn/chushidongtai/files/483439.asp.

Julia, C., Dingkuhn, M., 2013. Predicting temperature induced sterility of rice spikelets requires simulation of crop-generated microclimate. Eur. J. Agron. 49, 50–60.

Keating, B.A., Carberry, P.S., Hammer, G.L., Probert, M.E., Robertson, M.J., Holzworth, D., Huth, N.I., Hargreaves, J.N., Meinke, H., Hochman, Z., 2003. An overview of APSIM, a model designed for farming systems simulation. Eur. J. Agron. 18 (3), 267–288.

Kohavi, R., 1995. A Study of Cross-Validation and Bootstrap for Accuracy Estimation and Model Selection. Ijcai, Stanford, CA, pp. 1137–1145.

Krishnan, P., Swain, D., Bhaskar, B.C., Nayak, S., Dash, R., 2007. Impact of elevated CO2 and temperature on rice yield and methods of adaptation as evaluated by crop simulation studies. Agric. Ecosyst. Environ. 122 (2), 233–242.

Li, T., Hasegawa, T., Yin, X., Zhu, Y., Boote, K., Adam, M., Bregaglio, S., Buis, S., Confalonieri, R., Fumoto, T., 2015. Uncertainties in predicting rice yield by current crop models under a wide range of climatic conditions. Glob. Change Biol. 21 (3), 1328–1341.

Liu, B., Liu, L., Asseng, S., Zou, X., Li, J., Cao, W., Zhu, Y., 2016. Modelling the effects of heat stress on post-heading durations in wheat: a comparison of temperature response routines. Agric. For. Meteorol. 222, 45–58.

Liu, B., Liu, L., Tian, L., Cao, W., Zhu, Y., Asseng, S., 2014. Post-heading heat stress and yield impact in winter wheat of China. Glob. Change Biol. 20 (2), 372–381.

Mackill, D., Coffman, W., Rutger, J., 1982. Pollen shedding and combining ability for high temperature tolerance in rice. Crop Sci. 22 (4), 730–733.

Maruyama, A., Weerakoon, W.M.W., Wakiyama, Y., Ohba, K., 2013. Effects of increasing temperatures on spikelet fertility in different rice cultivars based on temperature gradient chamber experiments. J. Agron. Crop Sci. 199 (6), 416–423.

Matsui, T., Namuco, O.S., Ziska, L.H., Horie, T., 1997. Effects of high temperature and CO_2 concentration on spikelet sterility in indica rice. Field Crop Res. 51 (3), 213–219.

Matsui, T., Omasa, K., Horie, T., 2000. High temperature at flowering inhibits swelling of pollen grains, a driving force for thecae dehiscence in rice (Oryza sativa L.). Plant Prod. Sci. 3 (4), 430–434.

Matsui, T., Omasa, K., Horie, T., 2001. The difference in sterility due to high temperatures during the flowering period among japonica-rice varieties. Plant Prod. Sci. 4 (2), 90–93.

Matsui, T., Kobayasi, K., Nakagawa, H., Yoshimoto, M., Hasegawa, T., Reinke, R., Angus, J., 2014. Lower-than-expected floret sterility of rice under extremely hot conditions in a flood-irrigated field in New South Wales. Aust. Plant Prod. Sci. 17 (3), 245–252.

Matsushima, S., Ikewada, H., Maeda, A., Honma, S., Niki, H., 1983. Studies on rice cultivation in the tropics. Jpn. J. Trop. Agric. 27 (2), 98–106.

Matthews, R.B., 1995. Modeling the impact of climate change on rice production in Asia. Int. Rice Res. Inst.

Morita, S., Yonemaru, J.-I., Takanashi, J.-i., 2005. Grain growth and endosperm cell size under high night temperatures in rice (Oryza sativa L.). Ann. Bot. 95 (4), 695–701.

Nakagawa, H., Horie, T., Matsui, T., 2003. Effects of climate change on rice production and adaptive technologies, rice science: innovations and impact for livelihood. In: Proceedings of the International Rice Research Conference. Beijing, China, 16–19 September 2002. International Rice Research Institute (IRRI). pp. 635–658.

Nguyen, D.-N., Lee, K.-J., Kim, D.-I., Anh, N.T., Lee, B.-W., 2014. Modeling and validation of high-temperature induced spikelet sterility in rice. Field Crop Res. 156, 293–302.

Osada, A., Sasiprapa, V., Rahong, M., Dhammanuvong, S., Chakrabndhu, H., 1973. Abnormal occurrence of empty grains of indica rice plants in the dry, hot season in Thailand. Jpn. J. Crop Sci. 42 (1), 103–109.

Prasad, P.V., Craufurd, P., Summerfield, R., 1999. Fruit number in relation to pollen production and viability in groundnut exposed to short episodes of heat stress. Ann. Bot. 84 (3), 381–386.

Prasad, P.V., Pisipati, S., Mutava, R., Tuinstra, M., 2008. Sensitivity of grain sorghum to high temperature stress during reproductive development. Crop Sci. 48 (5), 1911–1917.

Prasad, P.V.V., Boote, K.J., Allen, L.H., Sheehy, J.E., Thomas, J.M.G., 2006. Species, ecotype and cultivar differences in spikelet fertility and harvest index of rice in response to high temperature stress. Field Crop Res. 95 (2–3), 398–411.

Redden, R.J., Hatfield, J.L., Prasad, V., Ebert, A.W., Yadav, S.S., O'Leary, G.J., 2013. Temperature, climate change, and global food security. pp. 181–202.

Sánchez, B., Rasmussen, A., Porter, J.R., 2014. Temperatures and the growth and

development of maize and rice: a review. Glob. Change Biol. 20 (2), 408–417.
Satake, T., Yoshida, S., 1978. High temperature-induced sterility in indica rices at flowering. In: Proceedings of the Crop Science Society of Japan. Japan.
Sherwood, S.C., Ingram, W., Tsushima, Y., Satoh, M., Roberts, M., Vidale, P.L., O'Gorman, P.A., 2010. Relative humidity changes in a warmer climate. J. Geophys. Res. 115 (D9).
Shi, C., Jin, Z., Tang, R., Zheng, J., 2007. A Model to Simulate High Temperature-Induced Sterility of Rice.
Shi, P., Tang, L., Lin, C., Liu, L., Wang, H., Cao, W., Zhu, Y., 2015a. Modeling the effects of post-anthesis heat stress on rice phenology. Field Crop Res. 177, 26–36.
Shi, P., Tang, L., Wang, L., Sun, T., Liu, L., Cao, W., Zhu, Y., 2015b. Post-heading heat stress in rice of South China during 1981–2010. PLoS One 10 (6), e0130642.
Shi, P., Zhu, Y., Tang, L., Chen, J., Sun, T., Cao, W., Tian, Y., 2016. Differential effects of temperature and duration of heat stress during anthesis and grain filling stages in rice. Environ. Exp. Bot. 132, 28–41.
Siebert, S., Ewert, F., Rezaei, E.E., Kage, H., Graß, R., 2014. Impact of heat stress on crop yield—on the importance of considering canopy temperature. Environ. Res. Lett. 9 (4), 044012.
Tanaka, W., Toriba, T., Hirano, H.-Y., 2014. Flower development in rice. In: Fornara, F. (Ed.), The Molecular Genetics of Floral Transition and Flower Development, pp. 221–262.
Tang, L., Zhu, Y., Hannaway, D., Meng, Y., Liu, L., Chen, L., Cao, W., 2009. RiceGrow: a rice growth and productivity model. NJAS Wagen. J. Life Sci. 57 (1), 83–92.
Tebaldi, C., Hayhoe, K., Arblaster, J.M., Meehl, G.A., 2006. Going to the extremes. Clim. Change 79 (3–4), 185–211.
Tian, X., Matsui, T., Li, S., Yoshimoto, M., Kobayasi, K., Hasegawa, T., 2010. Heat-induced floret sterility of hybrid rice (Oryza sativa L.) cultivars under humid and low wind conditions in the field of Jianghan Basin, China. Plant Prod. Sci. 13 (3), 243–251.
Ting, P., Qiang, L., Yafan, Z., Hongzheng, S., Yingchun, H., Yanxiu, D., Jing, Z., Junzhou, L., Linlin, W., Quanzhi, Z., 2015. Superior grains determined by grain weight are not fully correlated with the flowering order in rice. J. Integr. Agric. 14 (5), 847–855.
Wahid, A., Gelani, S., Ashraf, M., Foolad, M., 2007. Heat tolerance in plants: an overview. Environ. Exp. Bot. 61 (3), 199–223.
Wang, E., Martre, P., Zhao, Z., Ewert, F., Maiorano, A., Rötter, R.P., Kimball, B.A., Ottman, M.J., Wall, G.W., White, J.W., 2017. The uncertainty of crop yield projections is reduced by improved temperature response functions. Nat. Plants 3 (8), 17102.
Wassmann, R., Jagadish, S., Heuer, S., Ismail, A., Redona, E., Serraj, R., Singh, R., Howell, G., Pathak, H., Sumfleth, K., 2009. Chapter 2 climate change affecting rice production: the physiological and agronomic basis for possible adaptation strategies. Advances in Agronomy. Academic Press, pp. 59–122.
Yawei, W., Hua, Z.P.T., 2006. Extreme high temperatures in southern China in 2003 under the background of climate change. Meteorological 10, 003.
Yoshida, H., Horie, T., 2009. A process model for explaining genotypic and environmental variation in growth and yield of rice based on measured plant N accumulation. Field Crop Res. 113 (3), 227–237.
Yoshida, S., 1981. Fundamentals of rice crop science. Int. Rice Res. Inst.
Yoshimoto, M., Fukuoka, M., Hasegawa, T., Utsumi, M., Ishigooka, Y., Kuwagata, T., 2011. Integrated micrometeorology model for panicle and canopy temperature (IM2PACT) for rice heat stress studies under climate change. J. Agric. Meteorol. 67 (4), 233–247.
Zhang, B., Rui, W., Zheng, J., Zhou, B., Yang, F., Zhang, W., 2007. Responses of Pollen Activity and Seed Setting of Rice to High Temperature of Heading Period.
Zhang, G., Sakai, H., Tokida, T., Usui, Y., Zhu, C., Nakamura, H., Yoshimoto, M., Fukuoka, M., Kobayashi, K., Hasegawa, T., 2013. The effects of free-air CO_2 enrichment (FACE) on carbon and nitrogen accumulation in grains of rice (Oryza sativa L.). J. Exp. Bot. 64 (11), 3179–3188.
Zheng, J., Zhang, B., Chen, L., Du, Q., Qin, Y., Song, J., Zhang, W., 2004. Genotypic differences in effects of high air temperature in field on rice yield components and grain quality during heading stage. Jiangsu J. Agric. Sci. 21 (4), 249–254.